HHS Public Access

Author manuscript

J Vis Exp. Author manuscript; available in PMC 2021 June 09.

Application of Laser Microdissection to Uncover Regional Transcriptomics in Human Kidney Tissue

Daria Barwinska[1], **Michael J. Ferkowicz**[1], **Ying-Hua Cheng**[1], **Seth Winfree**[1,2], **Kenneth W. Dunn**[1], **Katherine J. Kelly**[1], **Timothy A. Sutton**[1], **Brad H. Rovin**[3], **Samir V. Parikh**[3], **Carrie L. Phillips**[4], **Pierre C. Dagher**[1], **Tarek M. El-Achkar**[1], **Michael T. Eadon**[1] **The Kidney Precision Medicine Project**

[1]Department of Medicine, Indiana University School of Medicine

[2]Department of Cellular & Integrative Physiology, Indiana University School of Medicine

[3]Division of Nephrology, Department of Medicine, Ohio State University Wexner Medical Center

[4]Division of Pathology, Indiana University School of Medicine

Abstract

Gene expression analysis of human kidney tissue is an important tool to understand homeostasis and disease pathophysiology. Increasing the resolution and depth of this technology and extending it to the level of cells within the tissue is needed. Although the use of single nuclear and single cell RNA sequencing has become widespread, the expression signatures of cells obtained from tissue dissociation do not maintain spatial context. Laser microdissection (LMD) based on specific fluorescent markers would allow the isolation of specific structures and cell groups of interest with known localization, thereby enabling the acquisition of spatially-anchored transcriptomic signatures in kidney tissue. We have optimized an LMD methodology, guided by a rapid fluorescence-based stain, to isolate five distinct compartments within the human kidney and conduct subsequent RNA sequencing from valuable human kidney tissue specimens. We also present quality control parameters to enable the assessment of adequacy of the collected specimens. The workflow outlined in this manuscript shows the feasibility of this approach to isolate sub-segmental transcriptomic signatures with high confidence. The methodological approach presented here may also be applied to other tissue types with substitution of relevant antibody markers.

Keywords

Biology; Issue 160; Laser Microdissection; LMD; protocol; kidney; glomerulus; tubular sub-segment

Correspondence to: Tarek M. El-Achkar at telachka@iu.edu, Michael T. Eadon at meadon@iupui.edu.

Disclosures

The authors have nothing to disclose.

Introduction

Technological advances in studying tissue specimens have improved understanding of the state of health and disease in various organs. Such advances have underscored that pathology can start in limited regions or in specific cell types, yet have important implications on the entire organ. Therefore, in the current era of personalized medicine, it is important to understand the biology at both the cell and regional level and not only globally[1]. This is particularly true in the kidney, which is composed of various specialized cells and structures that differentially initiate and/or respond to pathological stress. The pathogenesis of various types of human kidney disease is still not well understood. Generating a methodology to study changes in gene expression in specific tubular segments, structures or areas of the interstitium in the human kidney will enhance the ability to uncover region specific changes that could inform on the pathogenesis of disease.

Human kidney biopsy specimens are a limited and precious resource. Therefore, technologies interrogating transcriptomics in kidney tissue should be optimized to economize tissue. The available methods to study transcriptomics at the cell and regional level include single cell RNA sequencing (scRNaseq), single nuclear RNaseq (snRNaseq), in situ spatial hybridization, and laser microdissection (LMD). The latter is well suited for precise isolation of regions or structures of interest within tissue sections, for downstream RNA sequencing and analysis[2,3,4,5]. LMD can be adopted to rely on identification of specific cell types or structures based on validated markers using fluorescence-based imaging during dissection.

The unique features of laser microdissection assisted regional transcriptomics include: 1) the preservation of the spatial context of cells and structures, which complements single cell technologies where cells are identified by expression rather than histologically; 2) the technology informs and is informed by other imaging technologies because an antibody marker defines expression signatures; 3) the ability to identify structures even when markers change in disease; 4) detection of lowly expressed transcripts in approximately 20,000 genes; and 5) remarkable tissue economy. The technology is scalable to a kidney biopsy with less than 100 μm thickness of a core necessary for sufficient RNA acquisition and enables the use of archived frozen tissue, which are commonly available in large repositories or academic centers[6].

In the ensuing work, we describe the regional and bulk transcriptomics technology in detail, optimized with a novel rapid fluorescence staining protocol for use with human kidney tissue. This approach improves upon classic LMD explorations because it provides separate expression data for the interstitium and nephron sub-segments as opposed to aggregate tubulointerstitial expression. Included are the quality assurance and control measures implemented to ensure rigor and reproducibility. The protocol enables visualization of cells and regions of interest, resulting in satisfactory acquisition of RNA from these isolated areas to allow downstream RNA sequencing.

Protocol

The study was approved for use by the Institutional Review Board (IRB) at Indiana University.

NOTE: Use this protocol with kidney nephrectomy tissue (up to 2 cm in both the X and Y dimensions) preserved in the Optimal Cutting Temperature (OCT) compound and stored at −80 °C. Perform all work in a manner that limits RNA contamination, use clean disposable gloves and a face mask. Ensure the cleanliness of all surfaces. The equipment for which this protocol was optimized is a laser microdissection system featuring pulsed UV laser.

1. Cryosectioning

1. Expose 1.2 μm LMD PPS-membrane (poly(p-phenylene sulfide) slides to UV light (in a tissue culture laminar flow hood) for 30 minutes, immediately prior to cryosectioning. Store the slides at room temperature for optimal tissue adherence.
2. Cool the cryostat to −20 °C. Clean the work surfaces and install a new cutting blade.
3. Place a small slide box (cleaned with RNase surface decontamination solution) inside the cryostat chamber to store slides with freshly cut tissue.
4. Adhere the specimen in OCT to a tissue holder and allow it to equilibrate for a few minutes to reach the chamber temperature and strengthen the adhesion between the OCT block and the holder. Aid the process by using a heat extractor.
5. Cut the specimen to a thickness of 12 μm and affix it to the specialized LMD slide, using the slide adapter. Each slide holds one nephrectomy section per slide or up to two kidney biopsy sections per slide. Store the slides at −80 °C with a desiccant cartridge and inside a tightly closed plastic bag to prevent excess moisture from accumulating inside the slide box.
6. Label each slide with a specimen ID, date, and slide number.
7. Use the slides with specimens within 10 days from the initial date of cryosectioning.

2. Laser microdissection

1. Immediately before the staining, prepare the Antibody Mix (Ab-Mix) in 10% BSA in RNase-free PBS by adding the following: 4 μL of FITC-Phalloidin, 1.5 μL of DAPI, 2 μL of Tamm-Horsfall Protein (THP) antibody directly conjugated to Alexa Fluor 546, 3.3 μL of RNase Inhibitor, and 89.2 μL of 10% BSA in PBS (to reach a volume of 100 μL).

   NOTE: Alternative antibodies may be used in place of the THP antibody. For example, 2 μL of megalin/LRP2 antibody, directly conjugated to Alexa Fluor 568, can be used to label the proximal tubule. The Ab-Mix contains either LRP2

or THP antibody (to visualize either proximal tubules or thick ascending limbs, respectively). Other antibodies may be validated according to user needs.

2. Wash the slide in ice cold (−20 °C) 100% acetone for 1 min and move it to the humidity chamber.
3. Wash the top of the slide with RNase-free PBS for 30 s. Repeat.
4. Wash the top of the slide with 10% BSA in RNase-free PBS for 30 s. Repeat.
5. Apply the Ab-Mix for 5 min.
6. Wash the top of the slide with 10% BSA in RNase-free PBS for 30 s. Repeat.
7. Air dry the slide for 5 min and load it onto the laser microdissection cutting platform.
8. Install the collection tubes (autoclaved 0.5 mL microcentrifuge tubes) appropriate for PCR work, containing 50 µL of Extraction Buffer from the RNA isolation kit.
9. Proceed with LMD. Complete each LMD session within at most 2 hours.
    1. Collect pre- and post-LMD immunofluorescence images, using the microscope camera to validate the dissection for inter-operator variability as well as archival purposes, training and quality assessment of the performed protocol. In order to obtain 0.5 – 1 ng of RNA, a minimum of 500,000 μm^2 area is required. This often necessitates the use of up to 8 ×12 µm thick sections to obtain a sufficient amount of material for all sub-segments of interest.
    2. Identify regions of interest by staining, morphology and location and excise them using laser power greater than 40.

        NOTE: Here are the dissection criteria. The proximal tubule is defined by FITC-Phalloidin and LRP2 labeling. The thick ascending limb is defined by THP labeling. The collecting duct is defined by nuclear morphology (DAPI) and absence of other staining. The glomerulus is defined by FITC-Phalloidin and morphology. The interstitium is defined as the area between stained tubules.
10. Obtain a bulk cross-sectional expression signature by affixing two 12 µm sections to an LMD slide and dissecting the entire sections into extraction buffer.
11. Upon completion of the LMD process, close the collecting microcentrifuge tubes and flick it vigorously to ensure that the content moved from the cap to the bottom of the tube
12. Centrifuge the tubes at 3,000 × *g* for 30 s.
13. Incubate the tubes in 42 °C water bath for 30 min.
14. Centrifuge the tubes at 3,000 × *g* for 2 min.
15. Transfer the supernatant to a new 0.5 mL tube and store it in −80 °C.

3. RNA isolation

NOTE: For this RNA isolation protocol, we have adapted a protocol from a commercial RNA isolation kit. The manufacturer's protocol has been modified to meet the quality control requirements set for the project.

1. Add 250 µL of Conditioned Buffer (CB) to each RNA purification column (PC) and incubate for 5 min at room temperature.
2. Centrifuge all PCs for 1 min at 16,000 × *g*.
3. Add 50 µL of 70% ethanol (provided in the Kit) into the tubes with tissue samples. Mix the samples well by pipetting up and down. Do not vortex. Do not centrifuge.
4. Transfer the mixture into conditioned PCs and centrifuge for 2 min at 100 × *g* (to bind RNA), quickly follow with centrifugation for 30 s at 16,000 × *g* (to remove flow through). Repeat this step if more than 1 tube with tissue samples are available for any given sub-segment.
5. Add 100 µL of Wash Buffer 1 (WB1) into the PCs and centrifuge for 1 minute at 8,000 × *g*.
6. Prepare 40 µL of DNase per each sample (Add 5 µL of DNase to 35 µL of RDD buffer). Then add 40 µL of the mixture directly on the membrane of the PC and incubate for 15 min at room temperature.
7. Add 40 µL of WB1 onto the membrane of PC, and centrifuge for 15 s at 8,000 × *g*.
8. Add 100 µL of Wash Buffer 2 (WB2) onto the membrane of PC, and centrifuge for 1 min at 8,000 × *g*.
9. Add 100 µL of WB2 onto the membrane of PC, centrifuge for 2 min at 16,000 × *g*, immediately follow by centrifugation for 1 min at 16,000 × *g*.
10. Transfer the PC to a new 0.5 mL tube.
11. Add 12 µL of Elution Buffer (EB) onto the membrane and incubate for 7 min at room temperature. Thus, the final volume of all pooled dissected tissue samples is 12 µL per sub-segment.
12. Centrifuge the samples for 1 min at 1,000 × *g* and then for 2 min at 16,000 × *g*.
13. Transfer 2 µL into a fresh tube for Bioanalyzer analysis (to prevent freeze-thaw events).
14. Store all tubes in −80 °C until ready for further processing.

4. RNA sequencing

1. Assess each sample, intended for sequencing, for quality using a commercial Bioanalyzer and a chip dedicated to measuring small quantities of RNA.

2. Following quality control (QC) parameters prior to library prep and sequencing are required: Quantity of RNA greater than 4 ng for bulk and greater than 0.5 – 1 ng for each sub-segment; The percent of transcripts longer than 200 nucleotides (DV200) is required to be greater than 25% for LMD specimens (optimal > 75%).

3. Carry out library prep with a commercial cDNA library preparation kit intended for small quantities of degraded RNA. For the commercial kit listed in the supplement, we suggest using Option 2, which requires a minimum DV200 of 25% and no fragmentation. Some sequencing technologies may require higher minimum DV200 thresholds, such as 30%[7].

4. Add cDNA adapters and indexes.

5. Purify the RNAseq libraries using magnetic bead technology.

6. Deplete the ribosomal cDNA using a commercial rRNA removal kit prior to RNAseq library amplification step.

7. Purify the final RNAseq library using magnetic bead technology at a 2 ng/μL cDNA library concentration.

8. Carry out RNA sequencing of 75 bp paired end on a commercial sequencing system with 30 million reads/sample for bulk and 100 million reads/sample for sub-segmental sections.

9. Use a Reference RNA (25 μg) with every sequencing run to allow for control of batch effect. The initial concentration of our Reference RNA is 1 μg/μL, while the final concentration utilized in sequencing is 25 ng/μL. Run the reference RNA as a separate sample during library preparation and run with all LMD specimens each time.

10. Perform data analysis utilizing the FastQC application to assess the quality of sequencing, intergenic and mitochondrial reads and to determine reads attributed to a gene.

11. Use Integrative Genomics Viewer (IGV) for alignment and edgeR/rbamtools for transcript expression measures.

12. Remove samples with less than 100,000 reads. Quantile normalize the raw reads in the data set after filtering out lowly expressed genes at a user defined threshold.

13. Quantify the expression as a ratio of the sub-segment of interest to the average of all other sub-segments and log2-transform. Relative expression of the same gene may be compared across sub-segments and samples; however, it is not ideal to compare relative expression between two different genes due to potential differences in degradation across genes and RNA species.

14. Carry out an enrichment analysis to compare gene expression for a set of makers specific to each nephron sub-segment, while Reference RNA samples are compared across batches. A batch effect within 1 standard deviation of mean

expression with R value > 0.9 is considered acceptable. Additional normalization is required for a higher batch effect score. Any run that deviates from the accepted batch effect can be flagged. The Q30 should be greater than >90% for each sequencing run.

Representative Results

Samples

We present data from nine reference nephrectomies (3 specimens obtained at Indiana University and 6 specimens obtained through Kidney Precision Medicine Project), utilizing the rapid fluorescence staining protocol to isolate kidney nephron segments and interstitial areas. The sections utilized in this process were obtained from deceased kidney donors or unaffected tumor nephrectomies. These samples did not have pathologic evidence of disease as visualized in the H&E stain taken from contiguous sections (Figure 1A).

Laser Microdissection Quality Control

Identification of tubular sub-segments in the kidney is accomplished through antibody staining of unique tubular markers, as well as morphology and structural landmarks. Figure 1B–C illustrates the staining and microdissection of tubular sub-segments from a representative nephrectomy. This is accomplished by staining with DAPI (nuclei), FITC-Phalloidin (F-actin), and an additional antibody as necessary. The fluorescence staining used made it possible to visualize renal sub-segments with a high degree of confidence, further guided by morphological features as well as spatial positioning of the imaged structures (Figure 2). For example, glomeruli are revealed by phalloidin and DAPI staining with very distinctive morphology. Similarly, collecting ducts are visualized using nuclear morphology and the absence of other stains. The megalin/LRP2 antibody (directly conjugated to Alexa Fluor 568) is used here to identify proximal tubules. The thick ascending limb is visualized using a Tamm-Horsfall protein (THP) antibody (directly conjugated to Alexa Fluor 546). In contrast, the interstitium is excised along the outer membrane of the tubules and includes stromal and immune cells as well as small capillaries.

To obtain sufficient RNA of 0.5 – 1 ng per sub-segment, we seek to dissect a minimum area of 500,000 μm^2. This generally requires five to eight 12 μm thick sections (1 section per slide) to obtain sufficient material for all sub-segments. Dissection of any slide is completed in less than 2 hours to preserve RNA quality which allows one to cut ~4 segments per slide. Acquired tissue from the same sub-segment is pooled from multiple slides for downstream sequencing. A pre- and post-LMD immunofluorescence image is obtained to validate the collection of sub-segments of interest using an attached camera. Figure 3 delineates the success rates of dissection area and minimum RNA input. The success rate of meeting the minimum area input was >90% in this representative dataset. If the source tissue has a small amount of the CD or interstitium, there is a possibility the dissection area will be below 500,000 μm^2 for these segments after utilizing 8 slides. Additional slides could be cut depending on the needs of the user; however, as seen in Figure 3, if the area is close to 500,000 μm^2, the desired genes detected count has a high success rate (100%) and the total

read count success rate is 98.6% (1 specimen fell below the QC metric). Thus, there was enough tissue to achieve sufficient gene and read counts without utilizing additional tissue.

Sequencing Input Quality Control

The selected commercial library preparation and sequencing platform allows reproducible measurements of transcript expression, even with low quantities of highly degraded RNA. The minimum RNA input is 500 pg and the minimum DV200 (proportion of reads longer than 200 nucleotides in length) is above 25%. There is no minimum RIN. Sequencing with 100 million reads per sample, we seek to saturate the available reads in order to detect lowly expressed transcripts. The total reads can be adjusted according to the needs of the user.

It is straightforward to obtain sufficient RNA from two 12 μm bulk cross-sectional sections, so we seek to obtain a higher minimum total mRNA quantity of 4 ng for bulk sequencing. As delineated in the protocol, each sub-segment requires 0.5–1 ng in total RNA. The optimum RNA concentration is above 50 pg/μL after isolation. RNA amounts lower than this may lead to reduced gene detection and read counts observed. The majority of the samples yield >20,000 genes detected and >1 million reads. A DV200 greater than 25% for all specimens is required by the manufacturer (>75% is considered optimal). Although RIN is measured, the process of laser microdissection reduces RIN and the RNA sequencing platforms have been optimized for fragmented RNA. RNA quantity and quality are assessed by a bioanalyzer prior to sequencing. The rapid stain decreases the amount of time the tissue is exposed to room temperature and aqueous conditions, thereby minimizing to the extent possible, the degradation of RNA. The DV200 quality control metric for sequencing input is also found in Figure 3.

Sequencing Output Quality Control

Downstream data processing uses quantile normalization to allow comparison between samples in different batches. A minimum gene detection count of 10,000 and a minimum read count of 1 million are employed as thresholds to include samples in quantile normalization. Samples with lower gene detection or read counts are excluded from quantile normalization and subsequent comparative analyses. Only 1 out of 98 dissected sub-segmental samples failed to meet these thresholds (Figure 3). The Q30 (proportion of reads mapped at a 99.9% confidence) has been greater than 93% for each sequencing experiment (Figure 4).

We sequence a human reference RNA (25 ng) with each sequencing run to allow correction for batch effect if such correction is desired or required. The measured batch effect should be within 1 standard deviation of mean expression with an R value > 0.9. If batch effect is higher, additional normalization is required for that sequencing run. Here, the batch effect has been below 3% in the four sequencing experiments depicted in Figure 4. Thus, batch effect is typically addressed with quantile normalization for all sequencing runs, agnostic to the reference RNA. No correction based on the reference RNA has been implemented yet, but this information is available and could be used depending on the goals of a particular analysis.

Rigor and Reproducibility

It is important to demonstrate rigor in identifying cell types and structures. After laser microdissection, we test for the enrichment of known markers in the glomeruli, PT, TAL, CD, and interstitium as compared to the other compartments (Table 1). An enrichment analysis is used to compare gene expression for pre-determined expected markers. Gene expression is conveyed as $\log_2$ ratios of the expression of the sub-segment of interest compared to the mean of the other sub-segments. This expression metric was chosen for human samples as it reduces inter-individual variability, facilitating comparisons between cell and compartment types across specimens. However, the raw reads and quantile normalized reads may also be compared in alternative analyses. Figure 5 illustrates examples of immunohistochemical staining of these 5 selected known markers, as presented in the Human Protein Atlas.

Thus, we present orthogonal data sources which lend confidence to the correct sub-segment being collected: 1) the imaging which include the antibody stain and morphology of the segment/compartment, and 2) the expression output showing known markers are expressed in the corresponding sub-segment.

The regional transcriptomic analysis of genes expressed in each sub-segment allows for novel and underappreciated marker identification. Figure 6 illustrates an example of one marker for each sub-segment identified through LMD regional transcriptomics that also yielded a specific immunohistochemical staining of the corresponding nephron sub-segment.

To demonstrate reproducibility and understand the effect of operator variability, we conducted an experiment on a tumor nephrectomy sample. This specimen had the glomeruli, PT, and TAL re-dissected to increase the confidence of the RNA sequencing results and now serves as a useful technical replicate. Months apart, this sample underwent a second instance of cryosectioning, antibody staining, LMD dissection, RNA extraction, library prep, and RNA sequencing (Figure 7) of the glomeruli, PT and TAL compartments. The two versions (v1 and v2) were compared. The glomerular, PT, and TAL compartments were highly correlated with r^2 values >0.95, similar to the minimal batch effect of our reference RNA.

Discussion

LMD based transcriptomics is a useful technology that anchors gene expression to specific areas within the tissue. The basis of this technology and its potential application in the kidney has been described previously[8]. However, optimization, modernization and streamlining of fluorescence-based dissection specifically aimed at high accuracy dissection for downstream RNA sequencing is less ubiquitous. Because this methodology is spatially grounded within the tissue, it has the potential to reveal novel or underappreciated markers in tissue structures, especially in disease states. In fact, many common markers of cells may change with disease, hence relying only on the cell RNA expression markers for identity adjudication without the spatial context may be challenging in disease states. Therefore, the spatially anchored LMD approach is likely to complement and provide a ground-truth platform for many other transcriptomic technologies like single cell and single nuclear RNA sequencing, which define cells by predominantly by their gene expression profile[9].

Furthermore, the depth of gene expression provided by LMD (up to 20,000 genes per sample) provides another advantage and important venue to cross-link data from multiple sources and account for changes in gene expression that may not be apparent without a certain depth. The consideration of tissue economy is another positive feature of this technology, whereby a thickness of less than 100 μm total from a frozen block could be sufficient for an entire LMD dataset. This allows leftover tissue to be used for other analytical purposes.

The LMD has limitations. One anticipated limitation of laser microdissection transcriptomic data acquisition is its lower throughput nature. Future automation may prove important in improving scalability[10,11]. Two additional limitations of LMD transcriptomics include the dependency on expertise and the impact of tissue quality on data results. Inadvertent collection of cells and material outside the segment of interest is a known limitation because enriched compartments of cells are collected, not a single cell. LMD relies on a user's proficiency in understanding the tissue structure and therefore requires a certain domain expertise. Thus, individuals must be trained to identify relevant regions in the kidney with and without antibody staining. Finally, the effect of tissue quality may impact downstream data quality. The LMD protocol leads to tissue degradation, so the quality of starting material is important. However, this protocol was optimized on archived biopsies with several samples of only moderate quality. The data included shows that the selected transcriptomic platform is robust.

Of note, the isolation kit used and the downstream methodology of RNA sequencing must be tailored specifically for the expected degree of RNA degradation. The staining protocol described here was adopted because it had the most favorable effect on minimizing such effect. In this protocol, tissue was embedded in OCT in order to facilitate future comparisons across other transcriptomic technologies. However, formalin fixed tissue may be an alternative.

The data presented in this manuscript reveal the benefits of regional transcriptomics, including the optimization, quality control metrics and technology outcomes. The establishment of rigorous pre-analytical and analytical quality control criteria, and also the establishment of solid evidence of rigor and reproducibility is essential for any methodology. Future applications of regional transcriptomics can be broadly grouped into biologic applications, technical advancements, and analytic progress. Future biologic applications may be aimed at interrogation of tissue from uninjured, injured, and regenerating tubules, as well as tubules in close proximity to inflammation. These compartments can be identified in the same biopsy both by traditional morphological markers as well as antibody stains for "pathway" specific markers. The two antibody markers validated for use in this technology, megalin and uromodulin, are highly expressed in the proximal tubule and thick ascending limb respectively. However, it is possible that these markers may be reduced in severely diseased tissue. In these situations, additional antibody validation of pathway specific markers or novel markers that do not change their expression level may overcome this issue.

LMD is likely to be an appropriate method to use in transcriptomic interrogation of other organs. The selection and optimization of antibodies that work for rapid staining will be

imperative. An antibody that works in a regular staining protocol may not necessarily work for the rapid staining protocol, which likely requires high affinity antibodies. A primary conjugated antibody will minimize the steps needed and may offer advantages. However, conjugation of an antibody to fluorophores may alter the binding, and pilot experiments need to be performed before incorporation of these reagents in the protocol.

In conclusion, we describe a pipeline for fluorescence-based laser microdissection to isolate specific areas and structures in the human kidney to enable a transcriptomic analysis. This approach offers important advantages and can be extended to other tissues to provide a tissue based molecular interrogation. Regional transcriptomics complements other transcriptomic technologies by providing a histopathologic anchor to understand expression, assisting in the interpretation of the biology and the signature of health and disease. This technology fits naturally within the vision for building a transcriptomic atlas of the kidney.

Acknowledgments

General: The authors would like to thank the investigators of the Kidney Precision Medicine Project (www.kpmp.org) for their gracious support and advice.

Funding:

Support for this work was provided by the NIH/NIDDK K08DK107864 (M.T.E.); NIH/NIDDK UG3DK114923 (T.M.E., P.C.D.); R01DK099345 (T.A.S.). Research reported in this manuscript was supported by the National Institute of Diabetes and Digestive and the Kidney Diseases (NIDDK) Kidney Precision Medicine Project (KPMP), (www.kpmp.org), under award number U2CDK114886.

Data and materials availability: Data is archived in the Gene Expression Omnibus (GEO # pending)

References

1. El-Serag HB et al. Gene expression in Barrett's esophagus: laser capture versus whole tissue. Scandinavian Journal of Gastroenterology. 44 (7), 787–795 (2009). [PubMed: 19391063]
2. Kohda Y, Murakami H, Moe OW, Star RA Analysis of segmental renal gene expression by laser capture microdissection. Kidney International. 57 (1), 321–331 (2000). [PubMed: 10620215]
3. Murakami H, Liotta L, Star RA IF-LCM: laser capture microdissection of immunofluorescently defined cells for mRNA analysis rapid communication. Kidney International. 58 (3), 1346–1353 (2000). [PubMed: 10972700]
4. Woroniecki RP, Bottinger EP Laser capture microdissection of kidney tissue. Methods in Molecular Biology. 466 73–82 (2009). [PubMed: 19148600]
5. Noppert SJ, Eder S, Rudnicki M Laser-capture microdissection of renal tubule cells and linear amplification of RNA for microarray profiling and real-time PCR. Methods in Molecular Biology. 755 257–266 (2011). [PubMed: 21761310]
6. Amini P et al. An optimised protocol for isolation of RNA from small sections of laser-capture microdissected FFPE tissue amenable for next-generation sequencing. BMC Molecular Biology. 18 (1), 22 (2017). [PubMed: 28835206]
7. Catalytic FFPE Nucleic Acid Isolation for best NGS Performance. Retrieved from: https://celldatasci.com/products/RNAstorm/RNAstorm_Technical_Note.pdf (2016).
8. Micanovic R, Khan S, El-Achkar TM Immunofluorescence laser micro-dissection of specific nephron segments in the mouse kidney allows targeted downstream proteomic analysis. Physiological Reports. 3 (2) (2015).
9. Lake BB et al. A single-nucleus RNA-sequencing pipeline to decipher the molecular anatomy and pathophysiology of human kidneys. Nature Communications. 10 (1), 2832 (2019).

10. Rodriguez-Canales J et al. Optimal molecular profiling of tissue and tissue components: defining the best processing and microdissection methods for biomedical applications. Methods in Molecular Biology. 980 61–120 (2013). [PubMed: 23359150]

11. Hipp JD et al. Computer-Aided Laser Dissection: A Microdissection Workflow Leveraging Image Analysis Tools. Journal of Pathology Informatics. 9 45 (2018). [PubMed: 30622835]

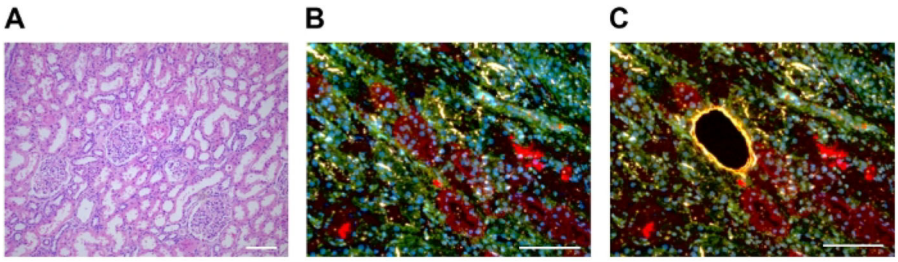

Figure 1: Representative images of the renal tissue.

(**A**) H&E stain of a human reference kidney tissue. (**B**) Immunofluorescent image of human reference kidney tissue with stained thick ascending limb segments prior to LMD and (**C**) immediately following dissection of single thick ascending limb structure. Scale bar = 100 μm.

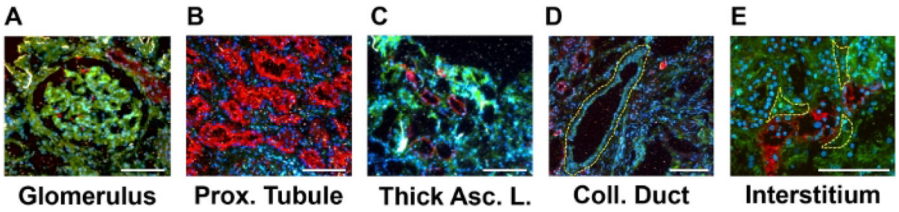

Figure 2: Representative images of reference renal sub-segments, visualized at 20x using a specific immunofluorescent staining approach.

(**A**)a Glomerulus, (**B**) Proximal Tubule, (**C**) Thick ascending limb, (**D**) Collecting duct, (**E**) Interstitium. (*= $p < 0.05$, **= $p < 0.01$, ***= $p < 0.001$ by ANOVA). Scale bar = 100 μm.

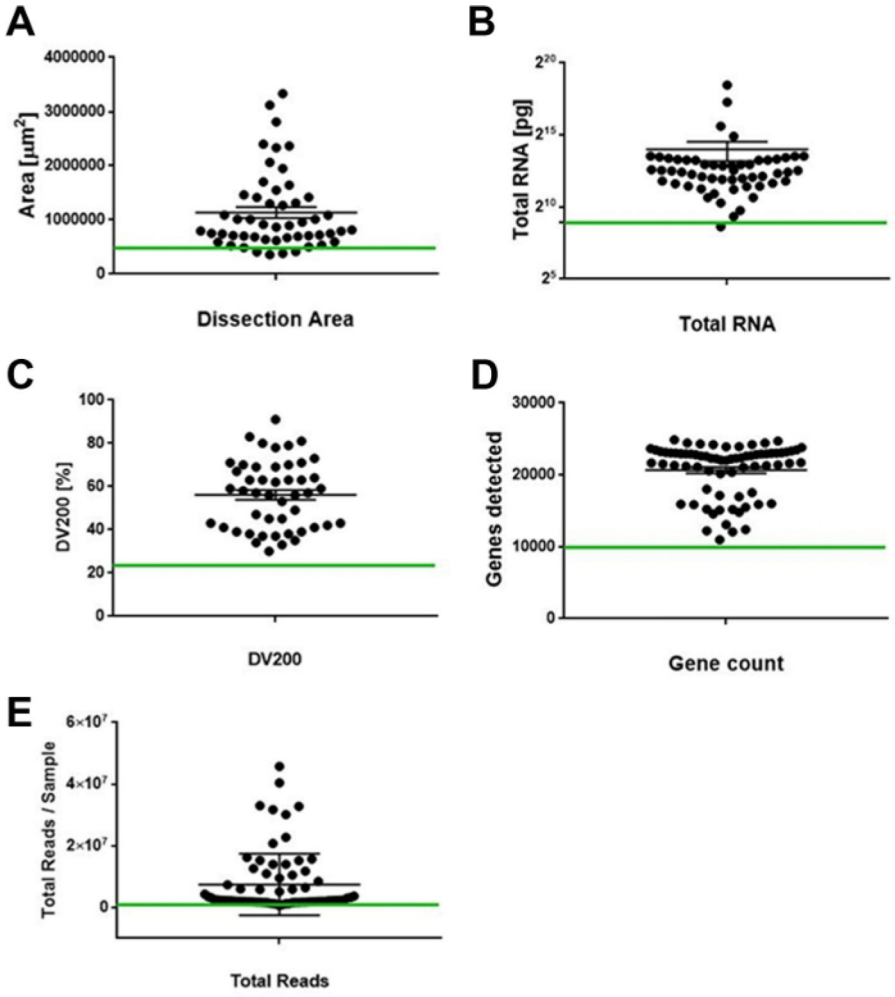

Figure 3: Quality control metrics in segmental transcriptomics.

(**A**) Greater than 90% of pilot samples met the dissection area input threshold of 500,000 µm^2. (**B**) All samples except one met the desired RNA input of at least 500 pg. (**C**) 100% of the pilot samples met the manufacturer's minimum DV200 threshold of 25% and (**D**) 100% of samples met our minimum threshold of 10,000 genes detected. (**E**) All samples except one reached a minimum total read count of 1 million. As expected, lower dissection areas correlate with reduced RNA concentrations, lower gene counts, and lower read counts.

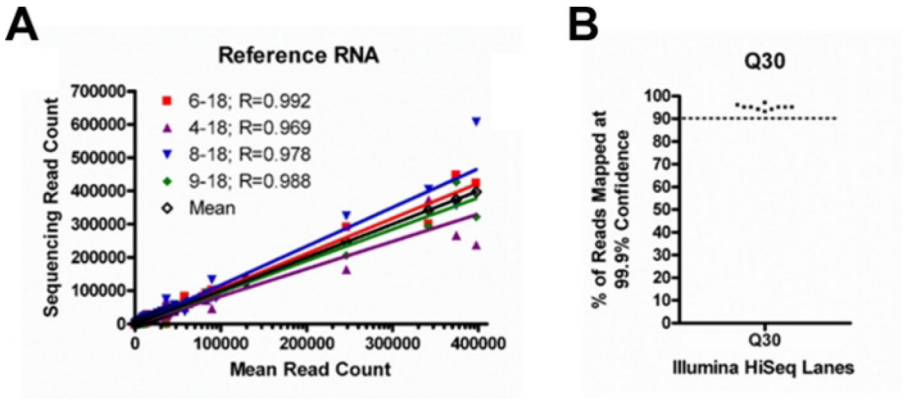

Figure 4: Sequencing Quality Control.

(**A**) Sequencing runs employing a reference RNA (not quantile normalized) are compared to mean expression of all runs. There is strong correlation with minimum batch effect (all R >0.969). (**B**) Greater than 93% of our reads in all runs were mapped with high confidence (Q30 or 99.9%). Note that Q30 values are provided on a per lane basis with multiple lanes per run.

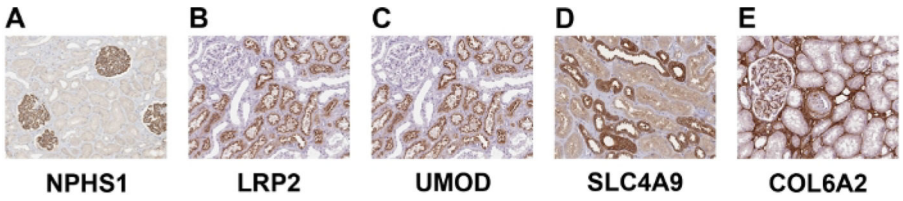

Figure 5: Examples of immunohistochemical staining to identify the selected known markers. Images are depicted for (**A**) NPHS1 (**B**) LRP2 (**C**) UMOD (**D**) SLC4A9 (**E**) COL6A2. Immunohistochemistry images are obtained from the Human Protein Atlas.

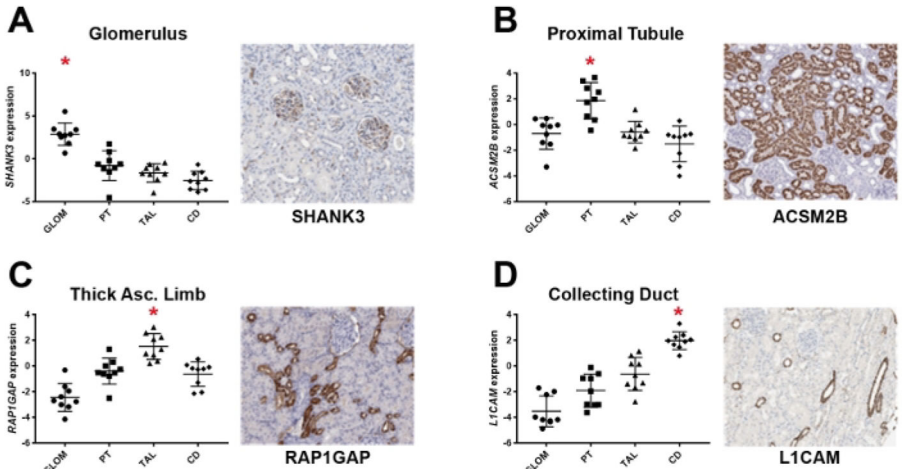

Figure 6: Examples of immunohistochemical staining to illustrate expression of nontraditional marker genes in relevant sub-segments.

Depicted transcripts with corresponding immunohistochemistry include (**A**) SHANK3 in glomerulus, (**B**) ACSM2B in proximal tubule, (**C**) RAP1GAP in the thick ascending limb, and (**D**) L1CAM in the collecting duct. Immunohistochemistry images are obtained from the Human Protein Atlas. (*= $p < 0.0001$ by ANOVA)

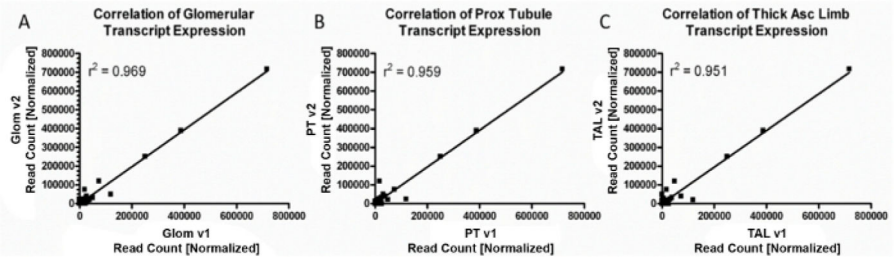

Figure 7: Correlation between two distinct dissections with separate sequencing of the same sample.

A high degree of correlation was observed between different dissections in the (**A**) glomerulus, (**B**) proximal tubule, and (**C**) thick ascending loop of Henle.

Table 1:

Representative average values for each sub-segment of interest among three nephrectomy samples, compared to the remaining sub-segments.

Marker	Segment	Fold Change	p-Value
NPHS1	Glomerulus	32.64	1.97E-08
LRP2	Proximal Tubule	4.69	1.21E-05
UMOD	Thick Ascending Limb	24.92	2.00E-07
SLC4A9	Collecting Duct	4.09	0.000133
COL6A2	Interstitium	7.19	1.47E-06